Science Advances

AAAS

advances.sciencemag.org/cgi/content/full/3/5/e1602670/DC1

Supplementary Materials for

Cryo-EM structure of human adenovirus D26 reveals the conservation of structural organization among human adenoviruses

Xiaodi Yu, David Veesler, Melody G. Campbell, Mary E. Barry, Francisco J. Asturias, Michael A. Barry, Vijay S. Reddy

Published 10 May 2017, *Sci. Adv.* **3**, e1602670 (2017)
DOI: 10.1126/sciadv.1602670

This PDF file includes:

- fig. S11. Structural conservation in protein VIII molecules from HAdV-D26 and HAdV-C5.
- fig. S12. Molecular clamping interactions by the protein VIII.
- fig. S13. β strand formation by the unidentified densities.
- fig. S14. Gluing interactions of the PPHs by protein VIII.
- fig. S15. Structures, locations, and organization of minor proteins relative to the MCPs in HAdV-D26.
- fig. S16. Structural similarities of the IIIa proteins from HAdV-D26 and HAdV-C5.
- fig. S17. Cryo-EM density and fit of the APD of IIIa in HAdV-D26.
- fig. S18. Gluing interactions involving IIIa, PPHs, and PB.

table S1. Number of amino acids and sequence identity between the respective capsid proteins in HAdV-D26 and HAdV-C5.

Protein	HAdV-D26	HAdV-C5	% Seq. Identity
Hexon	952*	952*	77
Penton base (PB)	519	571	74
Fiber	374	581	42
IIIa	560	585	78
VI	234	250	65
VIII	227	227	77
IX	134	140	47

*Number of amino acids in each protein.

table S2. Residues forming the HVRs in HAdV-D26 versus HAdV-C5.

HVR	HAdV-D26‡	HAdV-C5‡
HVR1	136-157§(22)¶	135-168§ (34)¶
HVR2	176-188 (13)	188-195 (8)
HVR3	205-213 (9)	212-220 (9)
HVR4	241-253 (13)	249-261 (13)
HVR5	260-281 (22)	268-284 (17)
HVR6	302-312 (11)	305-315 (11)
HVR7	417-453 (37)	419-453 (35)

§Start and end of amino acid residues in the respective HVRs. ¶Shown in parentheses are the number of residues in the respective HVRs. ‡The HVRs in HAdV-C5 were identified based on the previously published information. The positions of the HVRs in the HAdV-26 hexon were identified by aligning its amino acid (aa) sequence with that of the HAdV-C5 hexon and obtaining the ranges of residues in the corresponding HVRs.

table S3. Structural characteristics and interactions of the N and C termini of hexon subunits in HAdV-D26.

Hexon capsomer	Residues	Residues from Interacting proteins
Hexon-1A (PPH)	1-8 (NT)#1	58-66 (IIIa); 102-103, 517 (PB); 31-33 (PB-Sym)[§]
Hexon-1A (PPH)	947-951 (CT)β	β-strand with (938-943); 352-358 (Hexon-4K-Sym)
Hexon-1B (PPH)	2-10 (NT)#1	15-18, 182-186 (VIII-U)
Hexon-1B (PPH)	891-896	48-57 (IIIa); 92-98 (IIIa-Sym)
Hexon-1B (PPH)	946-950 (CT)β	β-strand with (938-943); 45, 95-99 (PB)
Hexon-1C (PPH)	4-7 (NT)#2	34-38 (VIII-U-Sym)
Hexon-1C (PPH)	891-896	19-22, 214-227 (VIII-U)
Hexon-1C (PPH)	946-949 (CT)x-!	720-724; 904-906 (CHEF-β-V2; Hexon-4K)
Hexon-2D	6-12 (NT)#2	101-106, 161-163 (VIII-U)
Hexon-2D	947-952 (CT)β	β-strand with (938-943); 353-359, 947-949 (Hexon-3G-Sym)
Hexon-2E	6-12 (NT)#2	No interactions
Hexon-2E	945-952 (CT)x-VIII	727-734, 888-895 (Hexon-1A); 102-107 (VIII-U)
Hexon-2E	937-941	105-110 (VIII-U) (strand)
Hexon-2F	5-9 (NT)#2	34-38 (VIII-V-Sym); 351-352, 949-952 (Hexon-3G-Sym)
Hexon-2F	945-950 (CT)x-UD	727-734, 891-894 (Hexon-3H)
Hexon-2F	937-941 (strand)	Unknown density (strand)
Hexon-3G	G6-G12 (NT)#2	101-104, 161-163 (VIII-V);
Hexon-3G	945-952 (CT)x-VIII	8-12 (Hexon-2F-Sym); 950-952 (Hexon-2D-Sym); 28-34 (VIII-V-Sym)
Hexon-3G	936-944 (strand)	28-36 (VIII-V-Sym) (strand)
Hexon-3H	6-14 (NT)#2	No interaction
Hexon-3H	945-952 (CT)x-VIII	727-734, 888-892 (Hexon-4J); 102-107 (VIII-V)
Hexon-3H	937-942 (strand)	105-110 (VIII-V) (strand)
Hexon-3I	2-13 (NT)#2	43-58 (VIII-V-Sym)
Hexon-3I	945-952 (CT)x-UD	728-734, 892-894 (Hexon-3I-Sym); 59-61 (Hexon-3H-Sym)
Hexon-3I	937-942 (strand)	Unknown density (strand)
Hexon-4J	2-13 (NT)#2	47-58 (VIII-U); 288-295(IIIa)
Hexon-4J	946-952 (CT)x-UD	729-734, 891-893 (Hexon-2F)
Hexon-4J	937-941 (strand)	Unknown density (strand)
Hexon-4K	2-10 (NT)#1	15-17; 80-82, 182-186 (VIII-V); 59-61 (Hexon-3I-Sym)
Hexon-4K	891-896	10-12, 58, 185-189, 193-194 (VIII-U); 286-288 (IIIa)
Hexon-4K	945-952 (CT)x-VIII	3-5, 28-34 (VIII-U); C8-C12 (Hexon-1C-Sym)
Hexon-4K	937-943 (strand)	29-36 (VIII-U) (Strand)
Hexon-4L	4-14 (NT)#2	No interactions
Hexon-4L	891-896	14-17, 72, 214-217, 224-227 (VIII-V)
Hexon-4L	947-950 (CT)x-!	662-664, 722-724, 902-904 (CHEF-β-V2; Hexon-3G-Sym)

[†]Interacting residues were identified based on a distance cutoff of 5Å.

[§]Sym refers to symmetry related molecule

#1 and #2 indicate two different conformations adopted by the N-termini (NT) of the hexon subunits.

The interactions involving the hexon NT are shown in white (blank) background.

"β" refers to the native β-strand formed between the C-terminal (CT) residues 946-950 and 948-943.

The interactions involving the hexon CT are shown in gray background.

"x-!" refers unfolded CT residues 946-950 and its interactions with CHEF strand of V2 barrel.

"x-VIII" refers unfolded CT residues 946-950 and its interactions with VIII molecule.

"x-UD" refers unfolded CT residues 946-950 and its interactions with unidentified density.

"(strand)" refers β-strand formation between the residues 948-943 and the respective residues listed. The interactions involving the hexon residues 891-896 are shown in dark gray background.

table S4. Fiber-PB interactions in HAdV-D26.

Fiber residues	Penton base residues
2-6	326-330
5-9	297, 324-328
11	215-216, 190 (Sym)[§]
14-16	446-448 (Sym), 196 (Sym)
15-17	285-286, 220-221
19-20	442, 448 (Sym)

[†]Interacting residues were identified based on a distance cutoff of 5Å.

[§]Sym refers to symmetry related molecule

table S5. Protein IIIa interactions with the major and minor proteins in HAdV-D26.

IIIa residues	Interacting residues (of the protein)
41-48	22-29 (VI)[¶]
14-23	18-27 (Hx1-A)
48-50	50-53 (Hx1-A)
51-59	1-17 (Hx1-A)
87-94	624-632 (Hx1-B)
94-95	932-934 (Hx1-B)
85-89	51-53 (Hx1-A-Sym)[§]
89-95	891-896 (Hx1-B-Sym)
100-104	6-8 (Hx1-A-Sym)
183-185	22-26 (Hx1-C-Sym)
284-289	54-59 (Hx4-J)
62-69, 103-107	32-37 (PB-Sym)[‡]
108-119	23-29 (PB-Sym)[‡]
331-336*	7-12 (Hx2-Sym-D)
374-378	894-897 (Hx1-A), 97-104 (VIII-U-Sym)
380-384	931-933 (Hx4-K)
385-390	38-46 (VIII-U)

[†]Interacting residues were identified based on a distance cutoff of 5Å.

¶ Shown in parenthesis are the interacting proteins. Hx and PB refer to proteins hexon and penton base and the numbers correspond to different hexons.

[§]Sym refers to symmetry related molecule

*The interactions in the shaded region involve residues in the appendage domain (APD).

[‡]Interactions involving the PB

table S6. Data collection and refinement statistics of HAdV-D26.

Data Collection	
Number of particles	19,590
Pixel size (Å)	1.31
Defocus range (μm)	0.8-3.0
Voltage (kV)	300
Electron dose ($e^-/Å^2$)	53
Map sharpening B-factor ($Å^2$)	-150
Refinement	
Resolution (Å)	20-3.7
Final R_{work}[§]	0.334
Final R_{free}[§]	0.336
Model Validation	
Ramachandran allowed (%)[‡]	91.9
Ramachandran generously allowed (%)[‡]	6.9
Ramachandran outliers (%)[‡]	1.1
RMSD	
Bonds (Å)	0.010
Angles (°)	1.8
Dihedral angles (°)	25.0
Improper angles (°)	1.17
PDB ID	5TX1

[§]Calculated using CNS.

[‡]Calculated using PROCHECK.

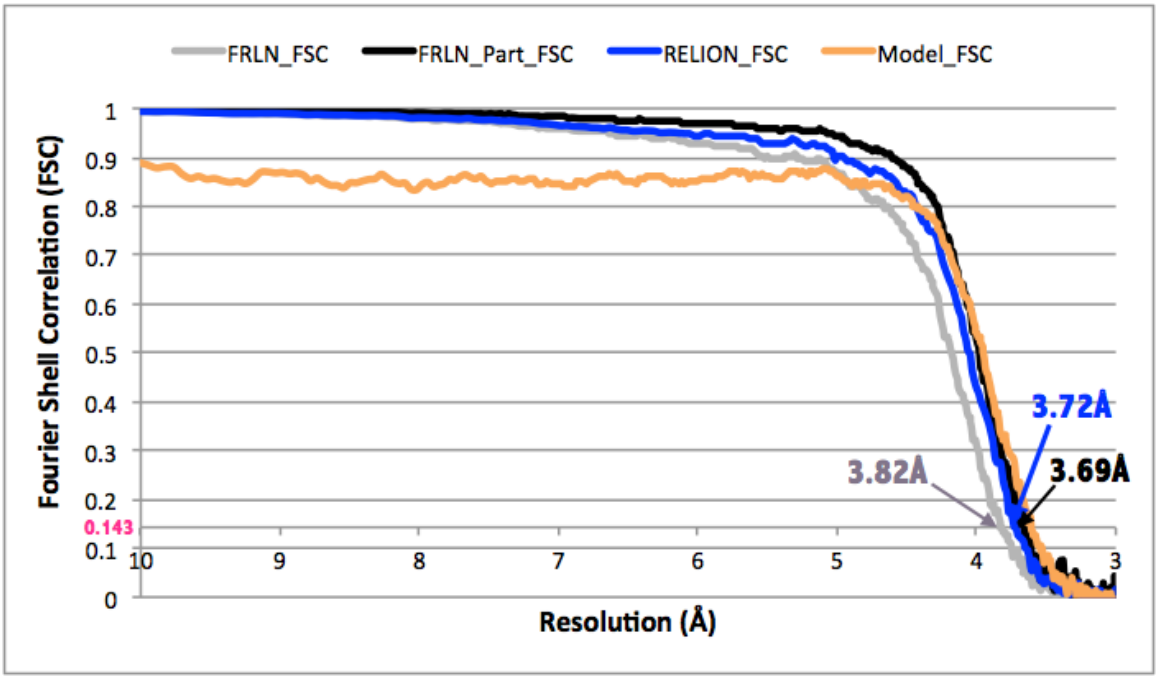

fig. S1. Resolution estimations of the cryo-EM reconstruction of HAdV-D26. The FSC curves as a function resolution (Å) obtained at the conclusion of refinements in Frealign, FSC (gray), Part-FSC (black) and from RELION is shown in blue. The resolution estimates according to the Gold-standard cutoff (FSC=0.143) are 3.82Å, 3.69Å and 3.72Å, respectively. Model to map FSC curve is shown in orange. A spherical mask with inner and outer radii of 280Å and 510Å, respectively was applied during the image reconstruction in Frealign.

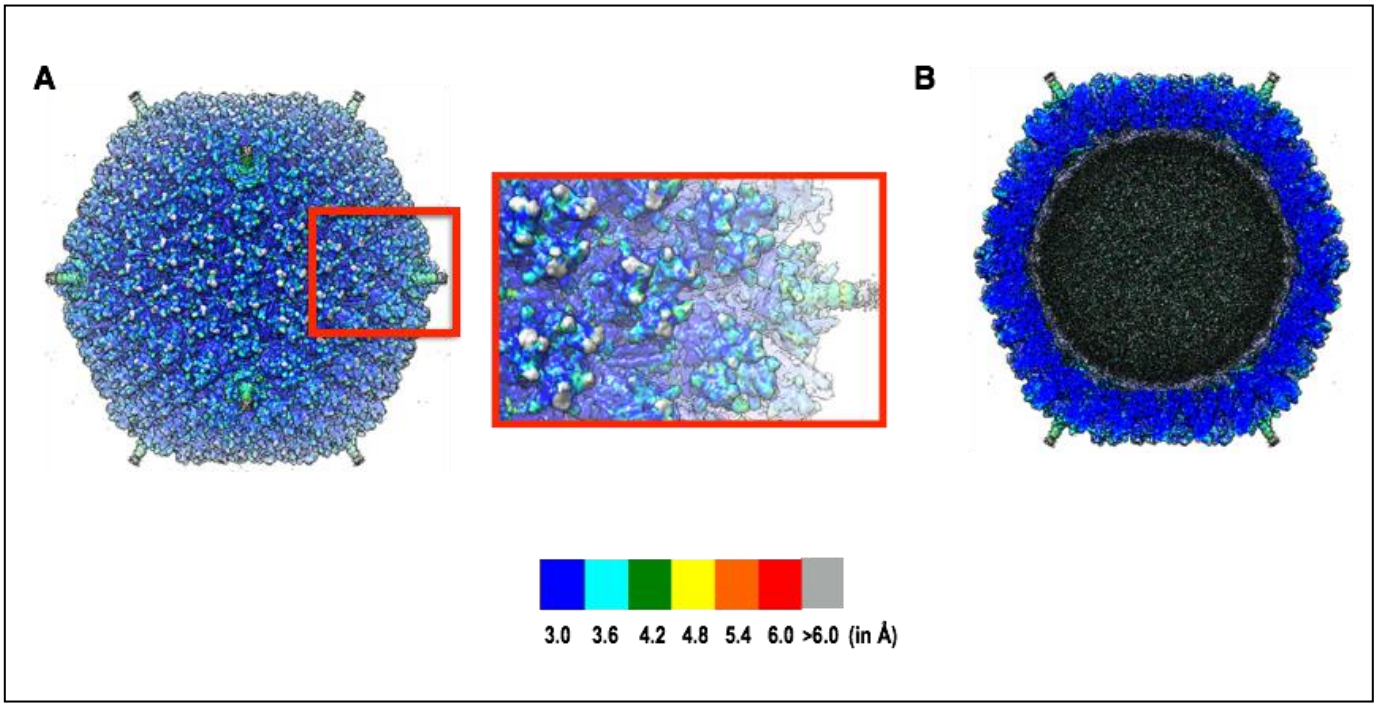

fig. S2. Estimation of local resolution of the HAdV-D26 cryo-EM reconstruction. (**A**) Surface presentation of HAdV-D26 cryo-EM reconstruction color coded according to the local resolutions, estimated using the program ResMap. The inset (red box) shows a zoom-in view of the map near the vertex region. Shown at the bottom are color codes for the resolution ranges generated by ResMap. (**B**) Cross section of the map showing that the resolution of the majority of the capsid shell is closer to 3.0Å, while the resolution limits for the fiber and the HVRs of hexon and penton base range between 3.6 and >6 Å. Knob region of the fiber is truncated.

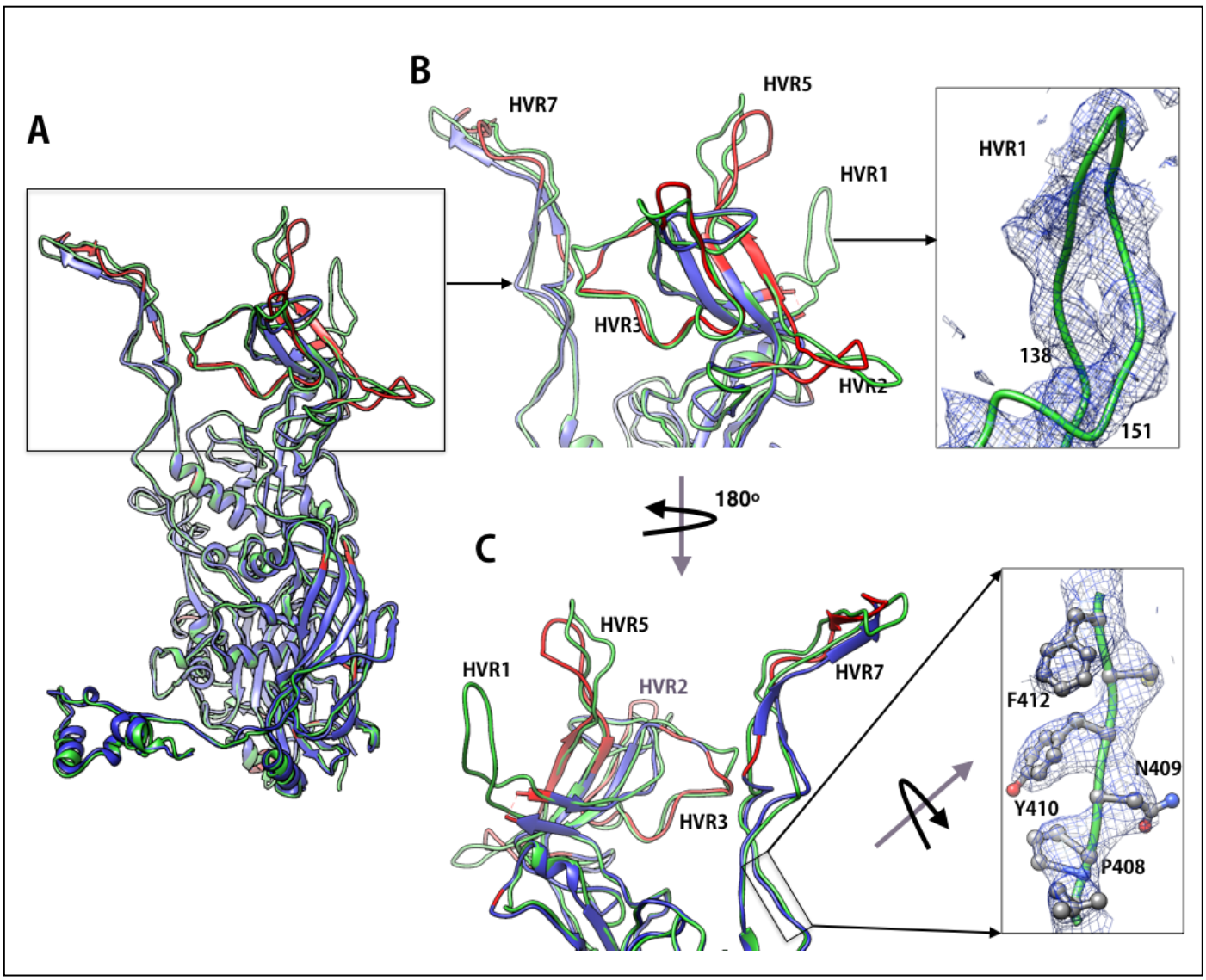

fig. S3. Structural similarities and differences between the hexon subunits of HAdV-D26 and HAdV-C5. (**A**) Superposition of hexon subunits from HAdV-D26 in green and HAdV-C5 (PDB-ID 3IYN) in blue. The regions of HAdV-C5 hexon that differ from that of HAdV-D26 by RMSDs > 2.0Å are shown in red and majority of these differences occur in the hyper-variable regions (HVRs). (**B**) A close up view of the HVRs and some of them are labeled. The inset shows the EM density of HVR1. (**C**) A rotated view of panel B. The inset shows the quality of the EM density in the hexon region leading into HVR7.

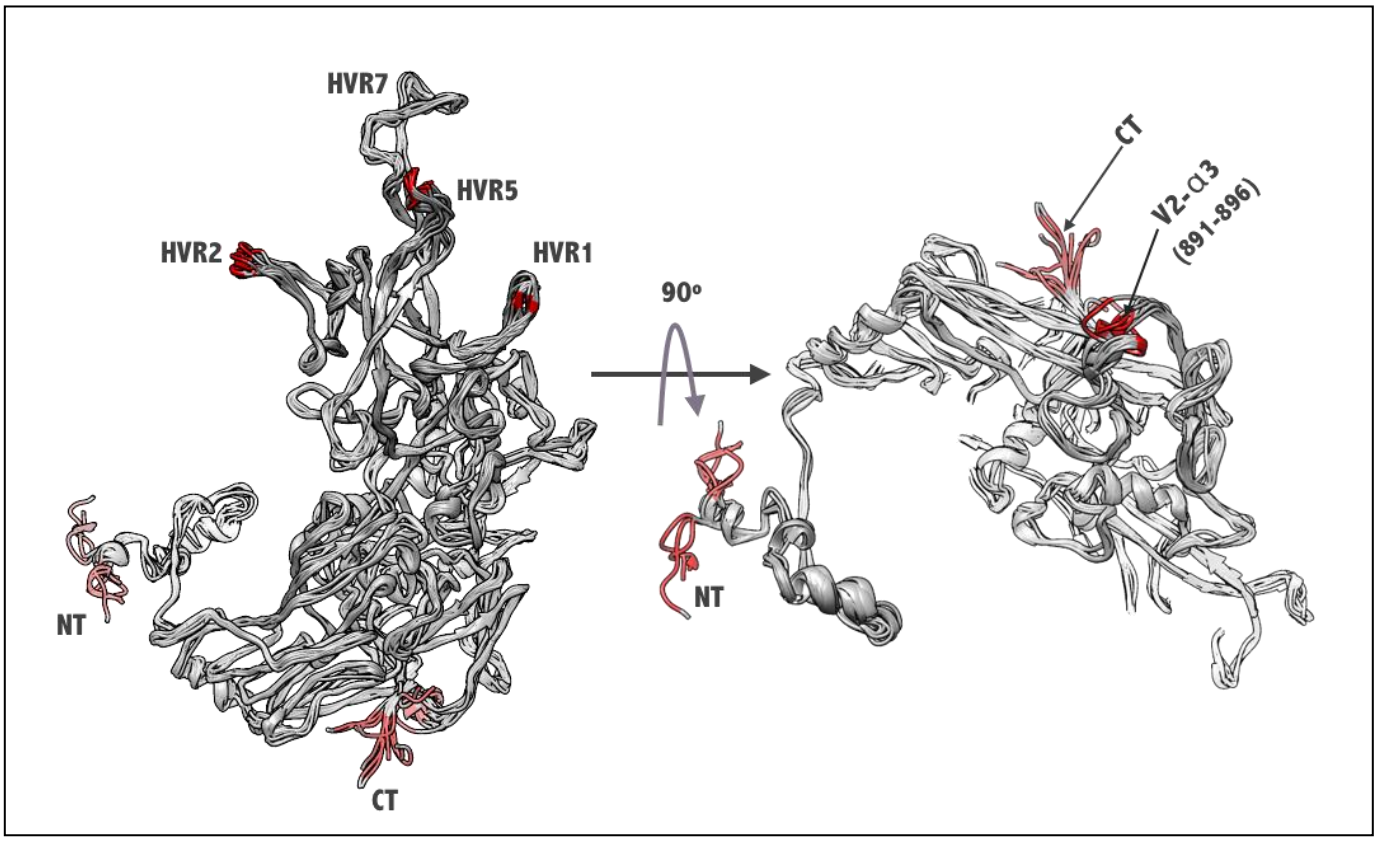

fig. S4. Structural similarities and differences between the different hexon structures in HAdV-D26. Shown on the left is the side view of superposition of 12 hexons that indicates virtually identical folds of the hexon subunits. The regions that differ greater than RMSD > 2.0Å (shown in red) are located at the N and C-termini as well as the HVRs. The RMSD values range between 0.6345 and 1.0Å for different superpositions. On the right is a 90° rotated view seen from the bottom (inside of the capsid). In addition to N and C-termini, the residues 891-896 also differ in their conformations in particular in A and B subunits in hexon-1 and J subunit in hexon-4, as they interact with the minor proteins IIIa and VIII.

A

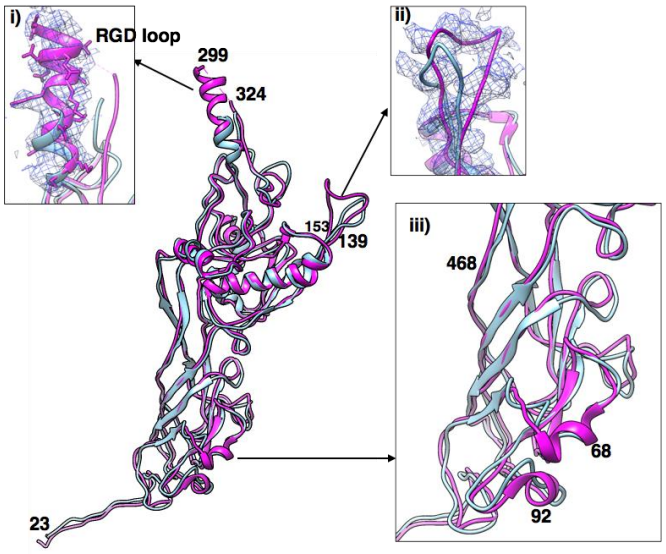

B

```
HAdV-C5_PB      MRRAAMYEEGPPPSYESVVSAAPVAAALGSPFDAPLDPPFVPPRYLRPTGGRNSIRYSEL
HAdV-D26_PB     -MRRAVVSSSPPPSYESVMAQ------------ATLEVPFVPPRYMAPTEGRNSIRYSEL
                  * *: ...********::              * *: *******: ** **********

HAdV-C5_PB      APLFDTTRVYLVDNKSTDVASLNYQNDHSNFLTTVIQNNDYSPGEASTQTINLDDRSHWG
HAdV-D26_PB     APQYDTTRVYLVDNKSADIASLNYQNDHSNFLTTVVQNNDFTPAEASTQTINFDERSRWG
                ** :************:*:****************:****::*.********:*:**:**

HAdV-C5_PB      GDLKTILHTNMPNVNEFMFTNKFKARVMVSRLPT------KDNQVELKYEWVEFTLPEGN
HAdV-D26_PB     GDLKTILHTNMPNVNEYMFTSKFKARVMVSRKHPEGVVETDLSQDKLEYEWFEFTLPEGN
                ****************:***.**********         . .* :*:***.********

HAdV-C5_PB      YSETMTIDLMNNAIVEHYLKVGRQNGVLESDIGVKFDTRNFRLGFDPVTGLVMPGVYTNE
HAdV-D26_PB     FSETMTIDLMNNAILENYLQVGRQNGVLESDIGVKFDSRNFKLGWDPVTKLVMPGVYTYE
                :*************:*:**:*****************:***:**:**** ******** *

HAdV-C5_PB      AFHPDIILLPGCGVDFTHSRLSNLLGIRKRQPFQEGFRITYDDLEGGNIPALLDVDAYQA
HAdV-D26_PB     AFHPDVVLLPGCGVDFTESRLSNLLGIRKKQPFQEGFRIMYEDLEGGNIPALLDVPKYLE
                *****::**********.**********:********* *:*************  *

HAdV-C5_PB      SLKDDTEQGGGGAGGSNSSGSGAEENSNAAAAAMQPVEDMNDHAIRGDTFATRAEEKRAE
HAdV-D26_PB     SKKKVEDETKNAA-----------------------AATADTTTRGDTFATPAQETAA-
                * *.  ::  ..*                          * : ******* *:*. *

HAdV-C5_PB      AEAAAEAAAPAAQPEVEKPQKKPVIKPLTEDSKKRSYNLISNDSTFTQYRSWYLAYNYGD
HAdV-D26_PB     ------------------DKKVEVLPIEKDESGRSYNLIQGT-HDTLYRSWYLSYTYGD
                               :**  : *: :*.. ******..    * ******:*.***

HAdV-C5_PB      PQTGIRSWTLLCTPDVTCGSEQVYWSLPDMMQDPVTFRSTRQISNFPVVGAELLPVHSKS
HAdV-D26_PB     PEKGVQSWTLLTTPDVTCGAEQVYWSLPDLMQDPVTFRSTQQVSNYPVVGAELMPFRAKS
                *:.*::***** *******:*********:**********:*:**:*******:*.::**

HAdV-C5_PB      FYNDQAVYSQLIRQFTSLTHVFNRFPENQILARPPAPTITTVSENVPALTDHGTLPLRNS
HAdV-D26_PB     FYNDLAVYSQLIRSYTSLTHVFNRFPDNQILCRPPAPTITTVSENVPALTDHGTLPLRSS
                **** ********.:***********:****.*************************.*

HAdV-C5_PB      IGGVQRVTITDARRRTCPYVYKALGIVSPRVLSSRTF*
HAdV-D26_PB     IRGVQRVTVTDARRRTCPYVYKALGIVAPRVLSSRTF*
                * ******:******************:**********
```

fig. S5. Structural superposition and sequence alignment of PBs from HAdV-D26 and HAdV-C5. (**A**) Structural superposition of the penton base (PB) subunits from HAdV-D26 (magenta) and HAdV-C5 (light blue, PDB-ID:3IYN). The PB subunits superpose well with an RMSD of 1.3Å for 443 Cα atoms (residues). Inset panel shows close-up views of i) fit of EM density of the helix (aa 282-299) leading to the (disordered) RGD containing loop, ii) fit of the β3-β4 loop with a 6 aa insertion and iii) superposition of the bottom β-barrel domain. (**B**) Amino acid sequence alignment of the PBs from HAdV-C5 and HAdV-D26 viruses, obtained by the CLUSTALW server (http://www.genome.jp/tools/clustalw/).

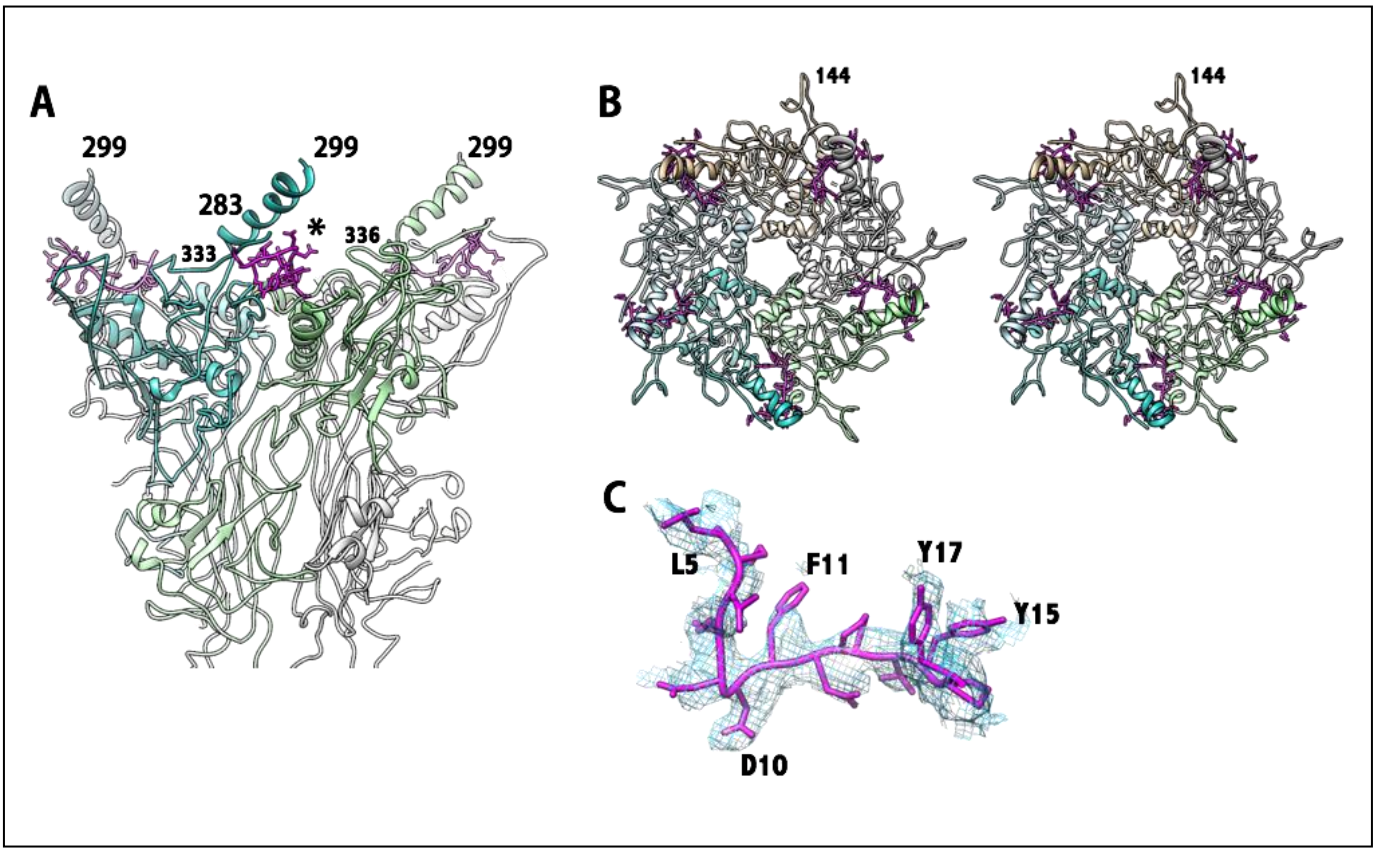

fig. S6. Interactions between the conserved N terminus of the fiber and the PB in HAdV-D26. (**A**) Side view of the pentameric PB interacting with the N-terminal residues (aa 2-20) of the fiber, which are shown in magenta and their location is identified by an asterisk. (**B**) A stereo view showing the top view of the 5 copies of NT of fiber interacting with the penton base. The observation of five copies of the N-terminal fiber peptide, as opposed to 3 copies is due to imposition of 5-fold symmetry as part of icosahedral symmetry during the particle reconstruction. In essence, only 3 of the 5 binding sites should be occupied. (**C**) Fit of the N-terminal fiber segment to the cryo-EM density.

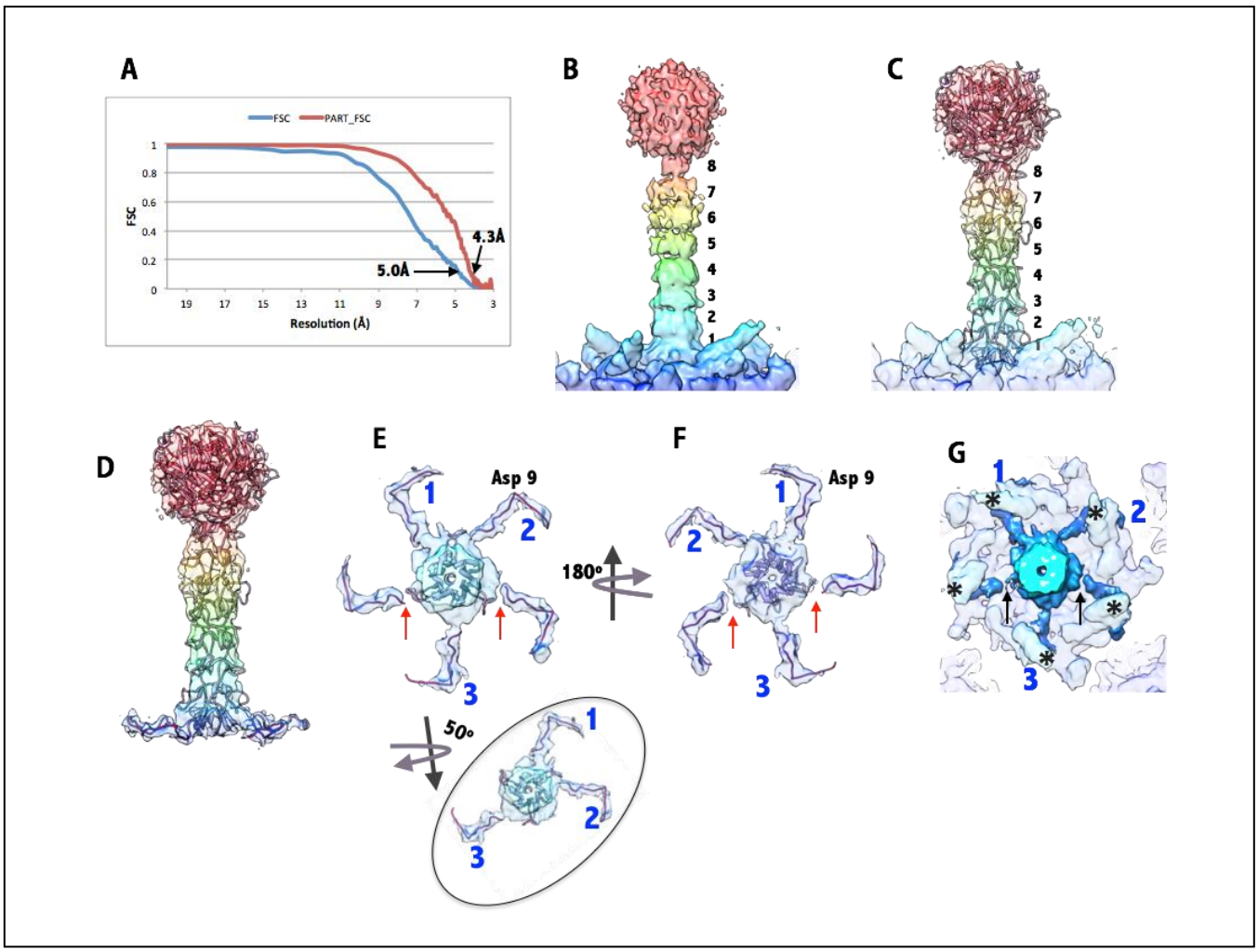

fig. S7. The structure and analysis of the fiber molecule obtained by LAR. (**A**) Shown on the top is the FSC (blue) or Part_FSC (red) vs. Resolution plot showing the nominal resolution of the localized asymmetric reconstruction of the Fiber-PB complex. (**B**) A color-coded side view of the fiber that highlights the fiber-shaft repeats, the knob domain is at the top and PB is at the bottom. Fiber shaft repeats (8) are labeled. (**C**) The fit of modified (extended) crystal structure of Ad2 fiber (PDB-ID:1QIU) into HAdV-D26 fiber density, using Chimera program. Different shaft repeats are labeled. (**D**) Extracted fiber density by subtracting the PB and PPH regions. (**E**) A cut away top view of the extracted fiber density (in panel D) highlighting the elbow shaped structures displayed by the fiber N-terminal tails (FNTs). The three fiber tails of the "fiber claw" that are connected to the central fiber density are labeled as 1, 2 and 3. The red arrows indicate the breaks in the EM density that occur in the remaining two FNTs. The backbone trace of the FNT model (residues 2-20) derived from high-resolution HAdV-D26 structure (fig. S6) is shown inside the elbow shaped densities. The Asp9 residue is located at the elbow bend. The oval-shaped inset shows the depiction of a 3-pronged fiber claw. (**F**) A 180° rotated view of the FNTs in panel E. (**G**) A top view showing the elbow shaped FNTs (dark blue) hooking the base of the protrusion that contains the RGD loop, identified by asterisks. The 3 prongs (1, 2 and 3) of the fiber claw are identified and the arrows indicate the break in the density of the remaining two FNTs.

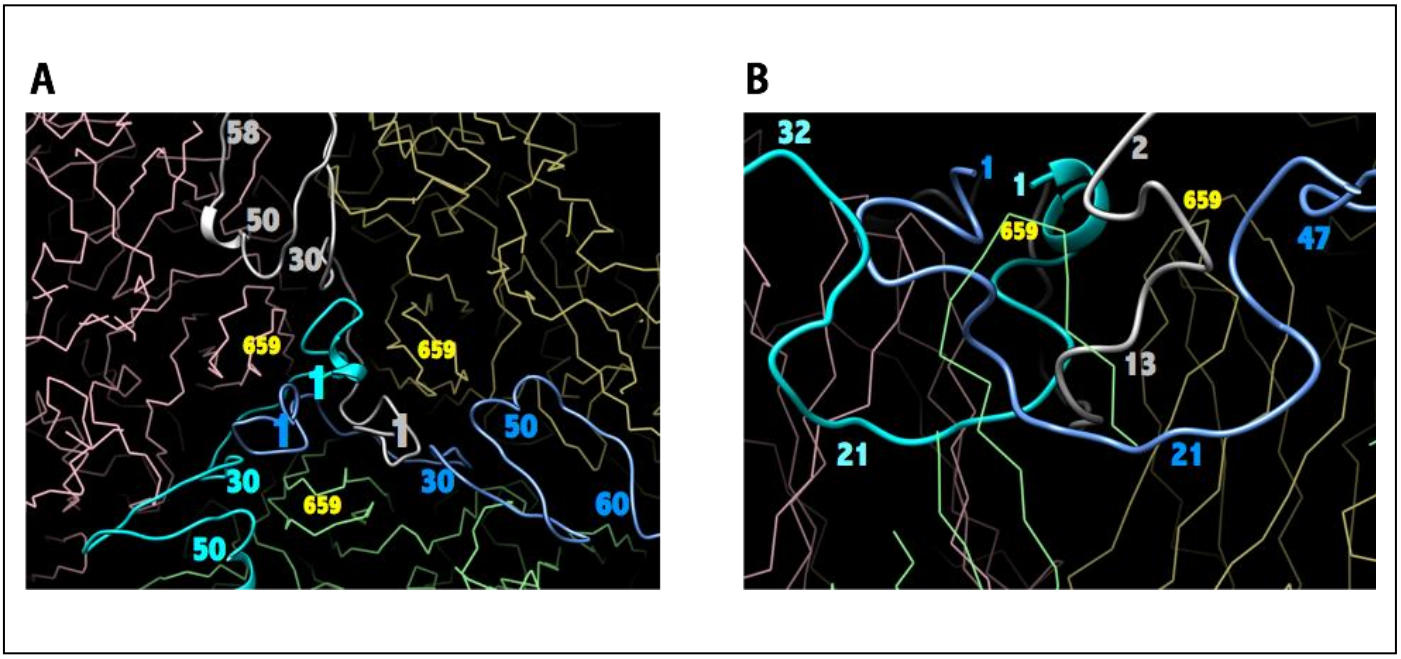

fig. S8. Interactions between the protein IX triskelions and the hexons. (**A**) Top view of the protein IX triskelions interacting with the hexon subunits at the local 3-fold axis. The residues 1-20 from each of three IX-polypeptides intertwine with each other with a left-handed twist at the 3-fold axes. The center of the triskelions interact with V2 domains of F, H, J hexon subunits at the local 3-fold axis, while with V2 domains of I subunits at the icosahedral 3-fold axis. (**B**) A side view of the triskelion seen embedded deep between the V2 domains of hexons.

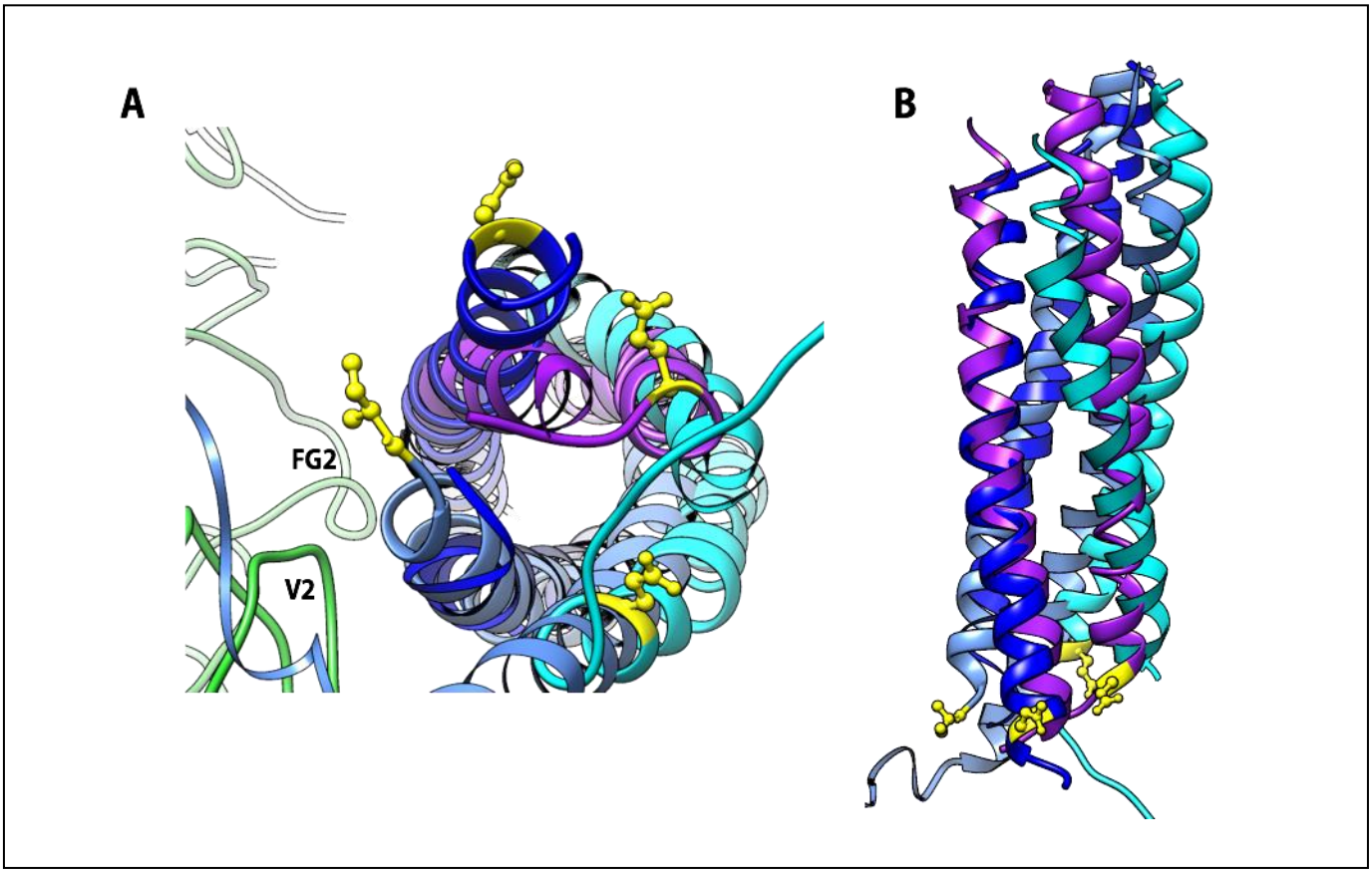

fig. S9. The structural overlay of the 4-HLXBs of IX from HAdV-D26 and HAdV-C5. (**A**) An end on view of the structural overlay of 4-HLXBs. A conventional structural superposition could not be done because of the multiple IX molecules involved and only certain regions of the IX polypeptides conform to the quasi 3-fold symmetry. Different colored helices correspond to the C-termini of structurally distinct IX molecules as described in Fig. 3. For example the blue colored helices are the anti-parallel helices that come from the neighboring facet, while the purple colored (parallel) helices belong the IX molecules that are located at icosahedral 3-fold axis. The set of helices identified with the yellow colored residues belong to HAdV-D26 and the cyan-colored helix corresponds to the fully ordered molecule of IX in HAdV-D26 structure. If the arrangement of the helices in both the 4-HXLBs is the same between the two viruses, then the same colored helices should overlap with each other. This is not the case, as the two blue colored (antiparallel) helices overlap with purple and light blue colored helices. In fact, no two helices of the same color overlap onto each other and their interactions with hexon neighbors are also different, indicating that the arrangement of helices in 4-HLXB is different between the HAdV-D26 and HAdV-C5 structures. (**B**) A side view of the superposition of helices.

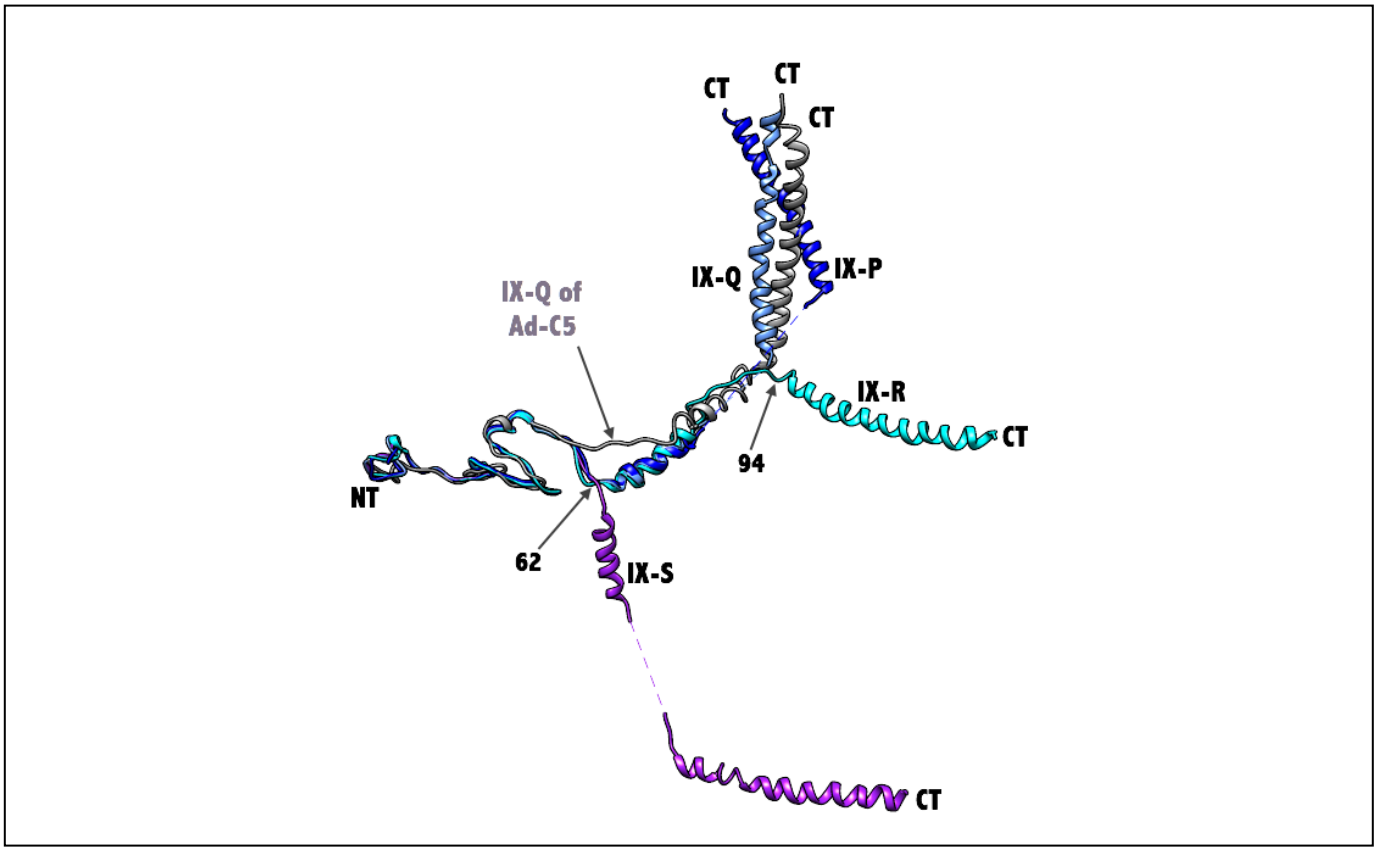

fig. S10. Structural superposition of the protein IX molecules. The triskelion forming region, containing residues (1-60), can be readily superimposed between different IX polypeptides in HAdV-D26 and even with that of the HAdV-C5 (Ad-C5) structure shown in gray. The color codes of the IX molecules of HAdV-D26 are the same as in Fig. 3. However, the structures of two of the IX molecules (R and S) branch out two different locations: 1) prior to the linker helix at residue 62 in the IX-S molecules, which are located at the icosahedral 3-fold axes and 2) at residue 94 located at base of coiled-coiled helices in the fully ordered IX-R molecule.

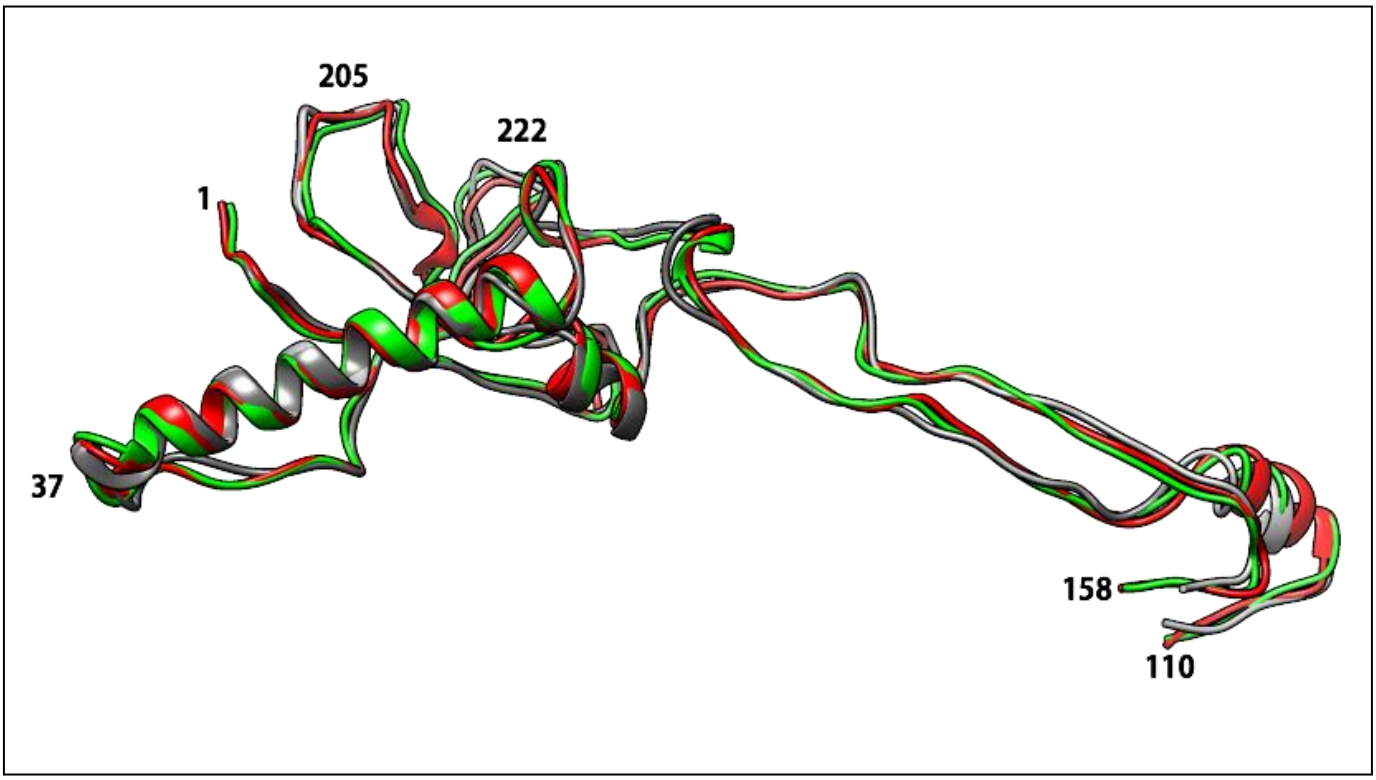

fig. S11. Structural conservation in protein VIII molecules from HAdV-D26 and HAdV-C5. Superposition of both the structurally distinct copies (red and green) of HAdV-D26 and from HAdV-C5 (gray, PDB-ID: 3IYN) highlights the structural equivalence of VIII molecules in HAdV-D26 and HAdV-C5 structures.

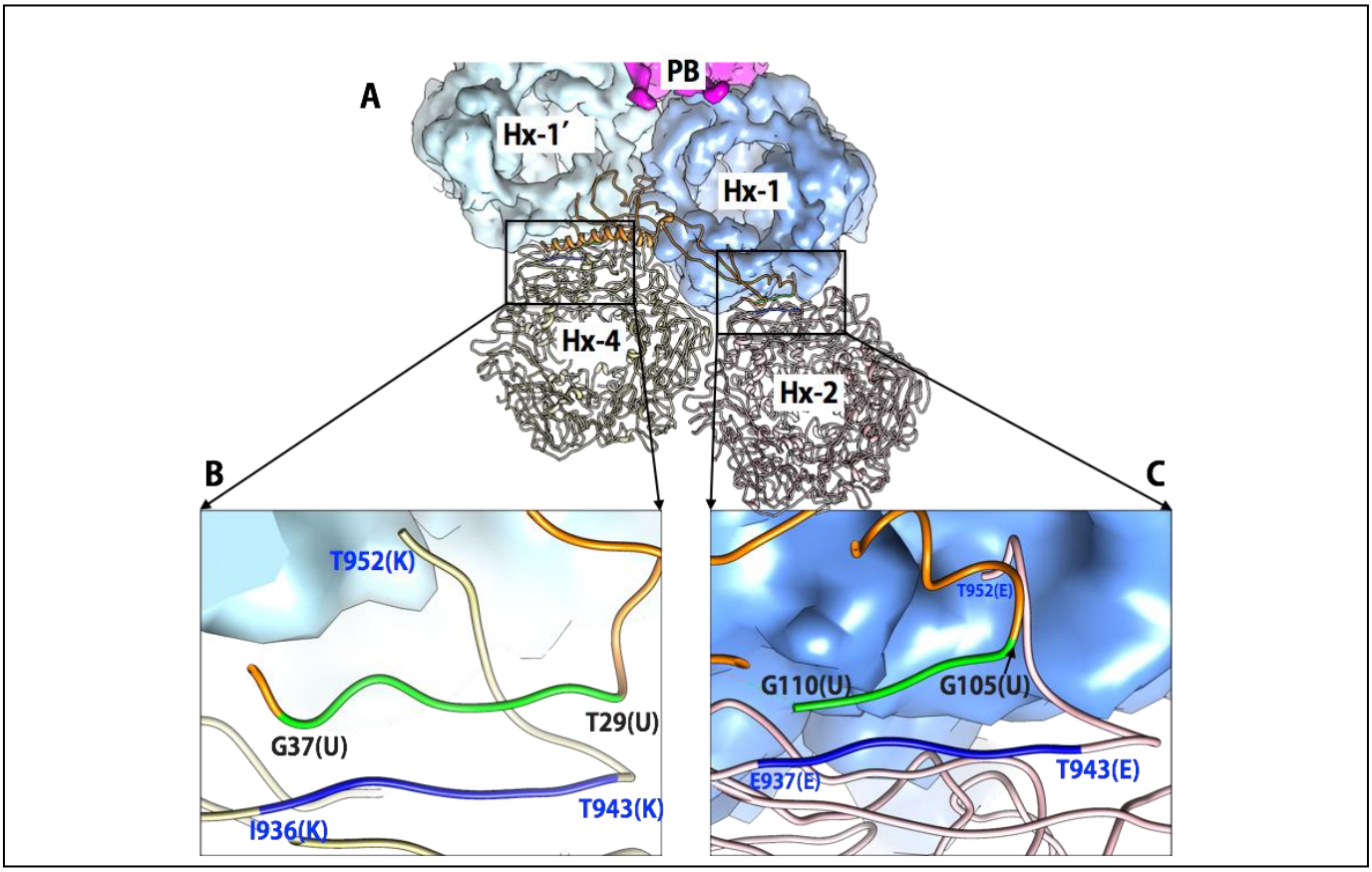

fig. S12. Molecular clamping interactions by the protein VIII. (**A**) The location of VIII-U (orange ribbon) molecule involved in clamping the hexons 2 (Hx-2) and 4 (Hx-4) (boxed regions) as well as gluing the neighboring peripentonal hexons (Hx1 and Hx1') together. (**B**) Close-up of the clamping interactions at one end that involve anti-parallel strand formation between the residues 29-37 (green) of VIII-U and 936-943 (blue) of K-subunit of Hx-4 by disrupting the native strand between residues 936-943 and 946-952 in the K-subunit. (**C**) The clamping interactions at the other end also involve anti-parallel strand formation between the residues 105-110 (green) of VIII-U and 937-943 (blue) of E-subunit of Hx-2 by disrupting the native strand between residues 937-943 and 946-952 in the E-subunit. Similar clamping interactions are formed by VIII-V molecule connecting Hx-3' and Hx-3 capsomers.

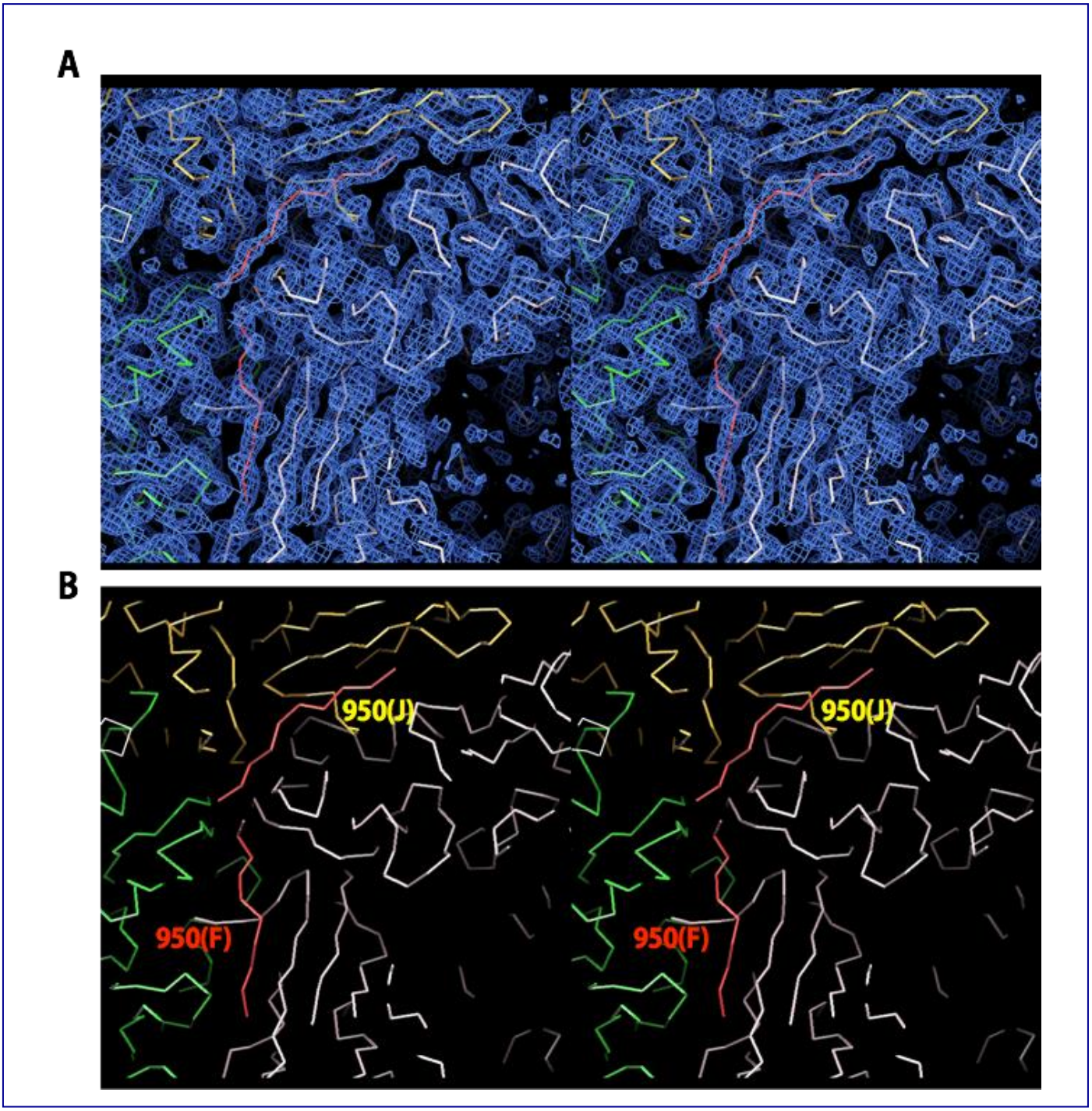

fig. S13. β strand formation by the unidentified densities. (**A**) Stereo diagram showing the β-strand formation by the unidentified densities surrounding the model segments shown in red with the hexon residues 936-943 in J (Hx-4) and F (Hx-2) subunits. These unidentified densities emulate the molecular clamping interactions by the VIII molecules depicted in fig. S12. (**B**) Stereo diagram as in panel A, without the EM density.

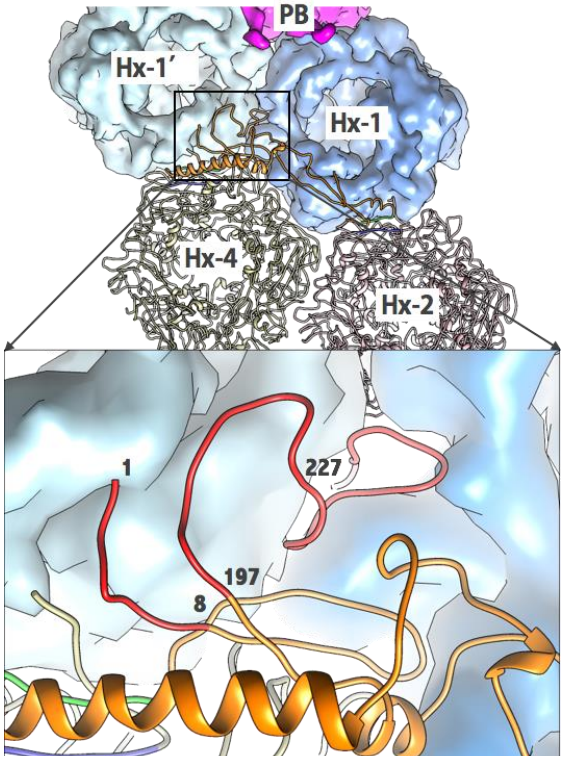

fig. S14. Gluing interactions of the PPHs by protein VIII. Shown on the top (boxed region) is the location of VIII-U involved in joining the adjacent peripentonal hexons (Hx-1 and Hx-1’) together at the vertex region. The location of PB (magenta) is identified. Inset shows the close-up view of the boxed region. The N-terminal (1-8) and C-terminal (197-227) regions of VIII-U (colored red) are involved in gluing the peripentonal hexons at the vertex region. These interactions, in conjunction with the interactions by IIIa molecules, are responsible for cementing the peripentonal hexons together and with the GONs (see fig. S18D). Similar interactions involving VIII-V molecule alone (no IIIa is present at this location) are responsible for mediating the interactions between the hexons, Hx-4 and Hx-2’ that belongs to an adjacent GON facet.

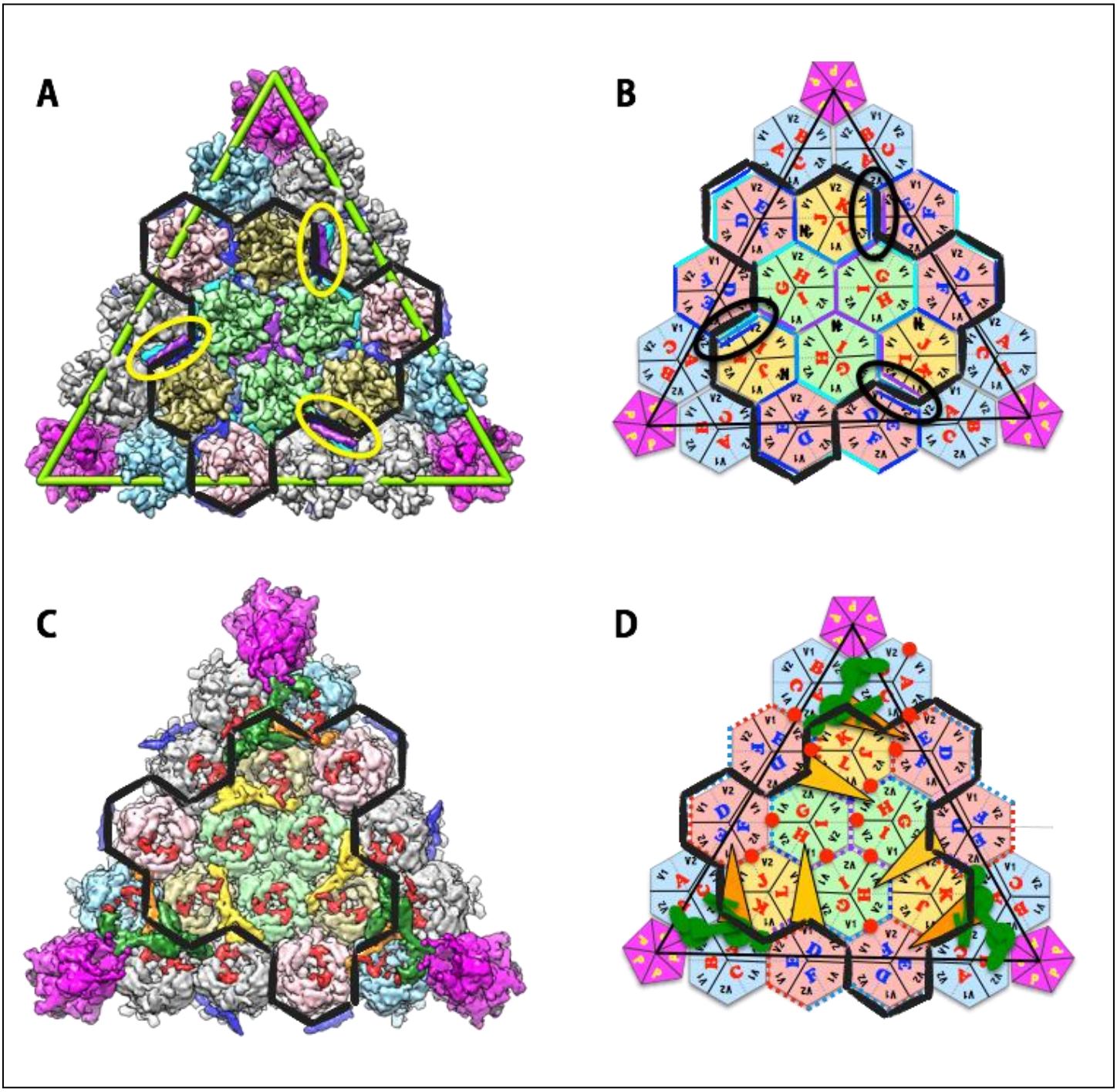

fig. S15. Structures, locations, and organization of minor proteins relative to the MCPs in HAdV-D26. (**A**) An icosahedral facet showing the exterior organization of major and minor capsid proteins in surface representation. Hexons are shown in light blue, pink, green, khaki and gray and the pentameric PBs are shown in magenta at the triangular corners (icosahedral vertices). The protein-IX triskelions seen in between the hexon subunits, primarily stabilize the group of nine hexons (GON) substructure, whose boundary has been identified by the trace of black sticks. The 4-HLXB structures,

identified by yellow ovals, are aligned with the boundaries of GON structures and mediate the inter-GON (inter-facet) interactions. Of note, each icosahedral facet (green triangle) should contain only 12 hexons (colored hexon trimers). We included six extra hexons (in gray) to completely fill the triangular facet. These gray colored hexons belong to the neighboring facets. (**B**) Schematic representation of the exterior organization of proteins illustrated in panel A. The hexons and PB are identified by hexagons and pentagons, respectively. In addition, the locations of the individual subunits and their V1 and V2 β-barrels that constitute respective hexons are labeled. The trace of protein IX are identified colored lines that border the hexagons. The locations of 4-HLXBs are identified by black ovals. The boundary of GON is identified by the thick back sticks. (**C**) An icosahedral facet showing the interior organization of major and minor capsid proteins. Protein IIIa is shown in green, while two distinct copies of VIII are shown in orange and yellow. The pVIn peptides bound in the hexon cavity are colored red. With exception of pVIn peptides, multiple copies of the same colored molecules are related to each other by the icosahedral symmetry. The boundary of GON is identified by the black sticks. Of note, all the VIII and IIIa molecules align the border of GON and PPHs that in turn mediate the inter-facet interactions. (**D**) Schematic representation of the interior organization of proteins illustrated as in panel C. The IIIa proteins are indicated by the green composite composed of spheres and sticks, while the VIII molecules are represented by two shades of orange colored obtuse triangles. The locations of pVIn peptides are identified red circles.

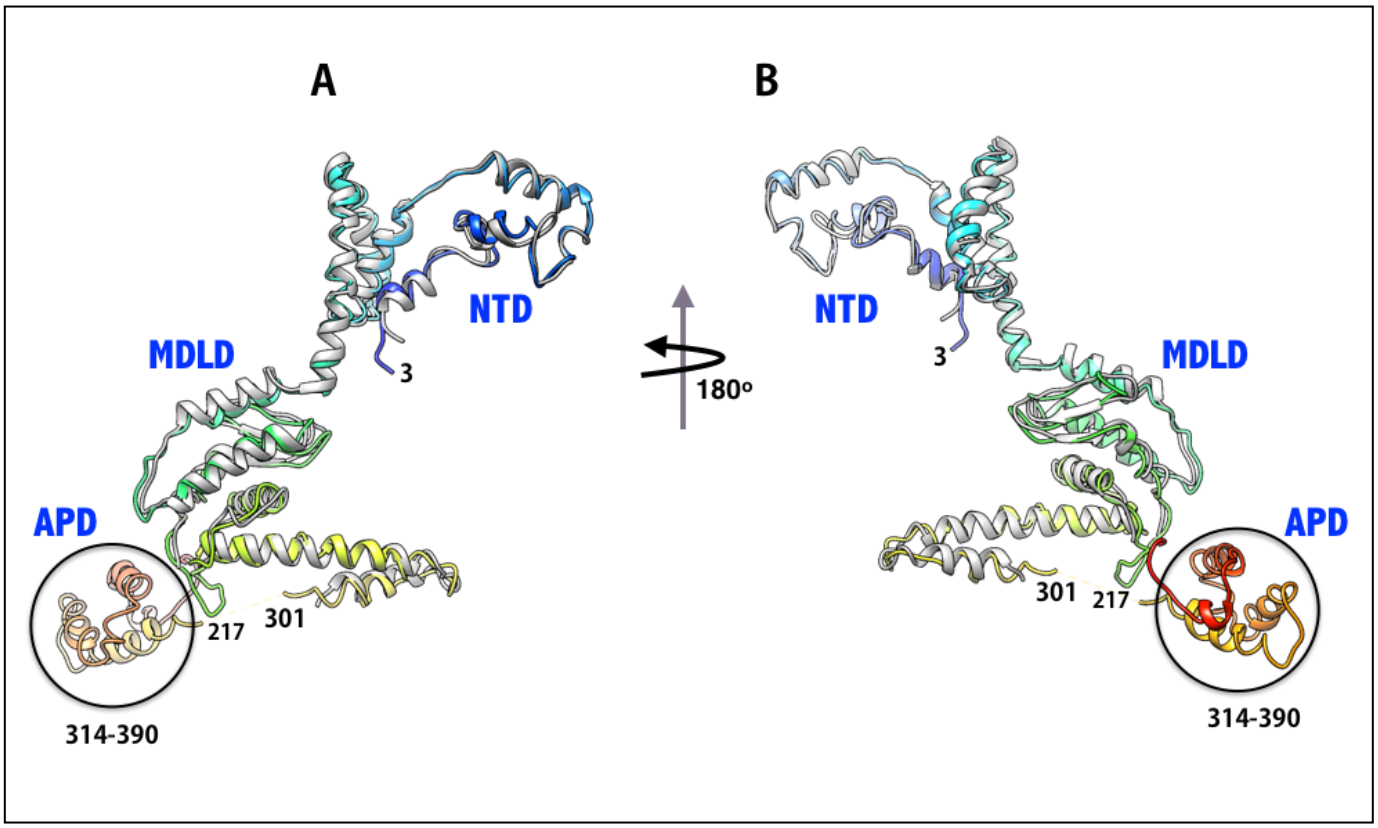

fig. S16. Structural similarities of the IIIa proteins from HAdV-D26 and HAdV-C5. (**A**) Structural superposition of ordered parts of IIIa in HAdV-D26 (rainbow colored) and HAdV-C5 (gray, PDB-ID: 3IYN). In the HAdV-D26 structure, we observed an extra helical domain, encircled, composed of residues 314-390. Different domains are identified. RMSD for the aligned regions between the two structures is 1.3Å. (**B**) A 180° rotated view of the panel A.

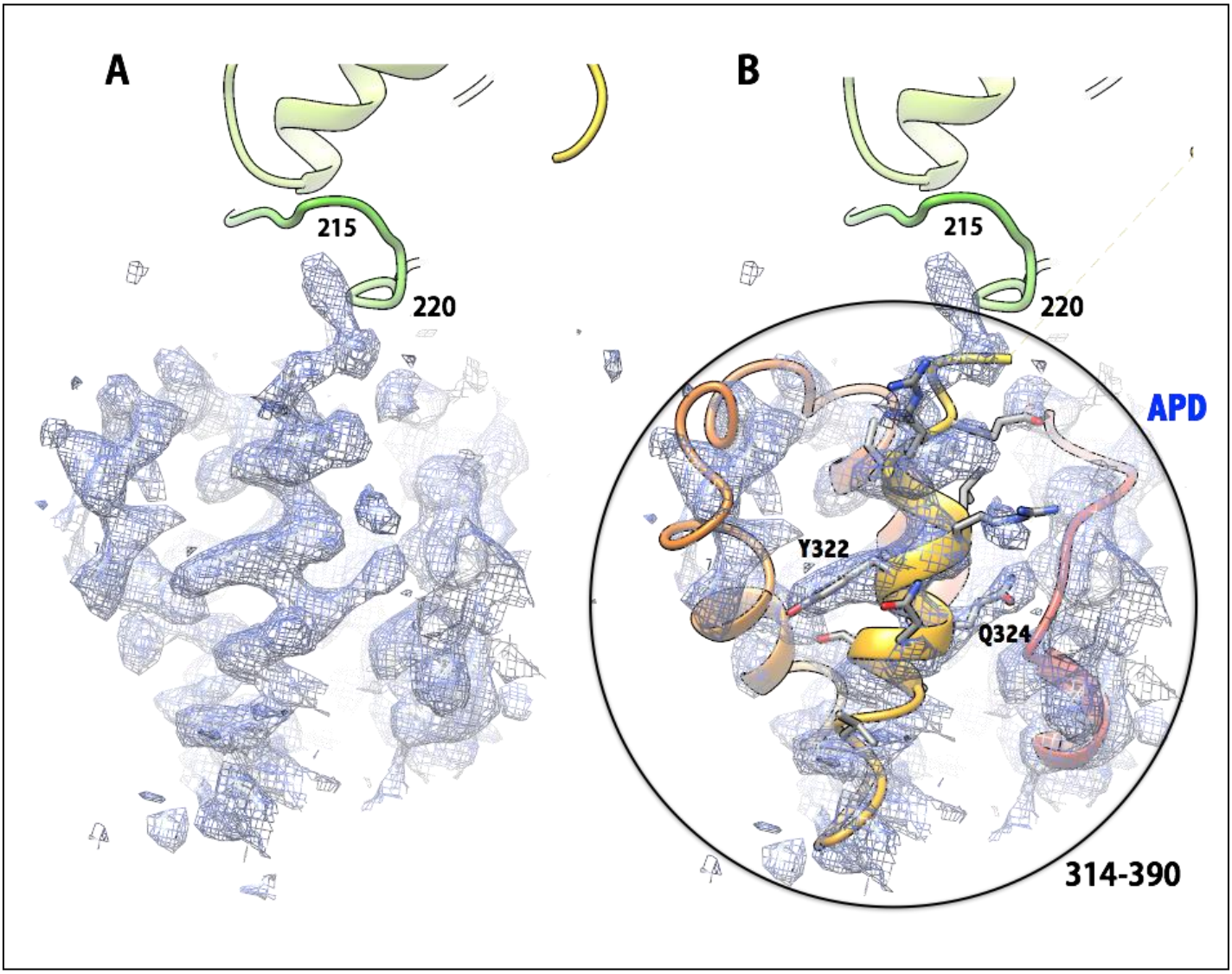

fig. S17. Cryo-EM density and fit of the APD of IIIa in HAdV-D26. (**A**) Extra density seen near residues 215-221 of IIIa (green ribbon). (**B**) Fit of the modeled region residues 314-390 to the EM density. The overall quality of the density in this region is relatively weak (modeled at 0.6σ) compared to the well-ordered regions (NTD, MDLD) of IIIa (modeled at 1.2σ). However, it was sufficient to assign sequence starting with the helix 314-332.

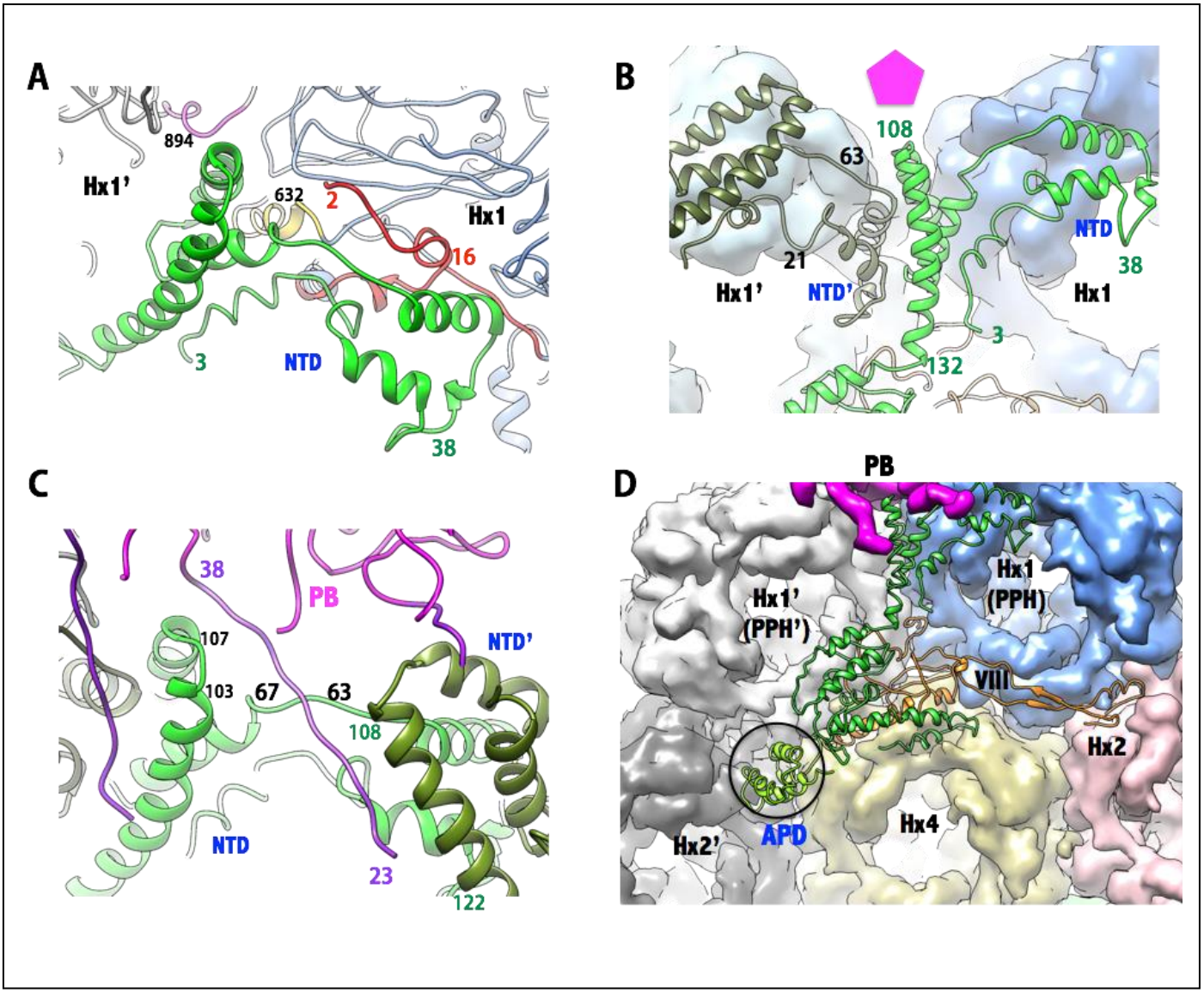

fig. S18. Gluing interactions involving IIIa, PPHs, and PB. (**A**) Close interactions between the NTD of IIIa with the N-terminal region (aa 1-30, A-subunit) of PPH (Hx1) and a few interactions with the region (aa 890-895, B-subunit) of the neighboring Hx1'. (**B**) Interactions between the NTDs of adjacent IIIa, which are colored in bright and dark shades green. Residues 82-104 of bright green copy interact closely with the residues 30-60 of the dark green copy of IIIa. These interactions are important for gluing the adjacent PPHs together underneath the vertex region. The location of the PB is identified by pentagon in magenta. (**C**) The ordered N-terminal region (aa 23-38) of PB interacts with residues 62-66, 103-107 of IIIa (bright green) and 108-118 of symmetry related copy of IIIa (dark green). (**D**) Diagram showing the bridging interactions mediated by VIII (orange) and IIIa (green) at the vertex region that glue the peripentonal hexons (Hx1 and Hx1') as well as Hx4 and HX2' from the adjacent group of nine hexon (GON) substructures together and as a larger group. The appendage domain (APD) of IIIa is circled. Of note, IIIa molecule overlays on top of the already bound VIII molecule and thereby further fortifying the cementing interactions between the adjacent PPHs and GONs.